Carbohydrate Polymers 87 (2012) 650–657

Contents lists available at SciVerse ScienceDirect

Carbohydrate Polymers

journal homepage: www.elsevier.com/locate/carbpol

# Characteristics and bending performance of electroactive polymer blend made with cellulose and poly(3-hydroxybutyrate)

Cai Zhijiang[a,b,*], Hou Chengwei[a], Yang Guang[a]

[a] School of Textiles, Tianjin Polytechnic University, Tianjin 300160, China
[b] Key Laboratory of Advanced Textile Composites, Ministry of Education of China, Tianjin 300160, China

ARTICLE INFO

*Article history:*
Received 4 May 2011
Received in revised form 5 July 2011
Accepted 16 August 2011
Available online 22 August 2011

*Keywords:*
Cellulose
Poly(3-hydroxybutyrate)
Bending displacement
Lifetime

ABSTRACT

This paper describes a novel cellulose/poly(3-hydroxybutyrate) blend based electroactive polymer. The fabrication process, bending actuation test and its characteristics are investigated. To prepare this new EAP, cellulose and PHB were dissolved in trifluoroacetic acid. The solution was cast to form a film followed by depositing thin gold electrode on both sides of the film. The characteristics of the cellulose/PHB film were investigated by Fourier transform infrared spectra, scanning electron microscopy, X-ray diffraction differential scanning calorimetry, tensile test and dynamic mechanical analysis. The bending performance was evaluated in terms of free bending displacement, electrical power consumption output and lifetime test under ambient conditions. Primary results show that this cellulose/PHB blend EAP is less sensitive to humidity and it shows higher bending displacement and longer lifetime than pure cellulose EAP at room humidity condition. These results indicate that this new cellulose/PHB blend EAP has potential for many biomimetic applications.



## 1. Introduction

Cellulose is a linear polymer made up of glucose molecules linked by β-(1-4)-glycosidic linkages. There are four principle sources of cellulose. The majority of cellulose is isolated from plants. A second source is the biosynthesis of cellulose by different microorganisms, including bacteria (*Acetobacter xylinum*), algae, and fungi among others. The other two less common sources include the enzymatic in vitro synthesis starting from cellobiosyl fluoride, and the chemosynthesis from glucose by ring-opening polymerization of benzylated and pivaloylated derivatives (Eichhorn et al., 2001; Takayasu & Fumihiro, 1997). As an environmentally friendly and renewable biomaterial, plant cellulose constitutes about $2 \times 10^{12}$ tons of the total annual biomass production photosynthesized by carbon dioxide fixation on land and in sea (Klemm, Heublein, Fink, & Bohn, 2005). Cellulose has been widely used in textile, food, paper, etc. Nowadays, lots of cellulose applications take advantage of its biocompatibility, hydrophilicity and chirality for the immobilization of proteins and antibodies for the separation of enantiomeric molecules as well as the formation of cellulose composite with synthetic polymers and biopolymer. As one of new applications, cellulose has been discovered as a smart material which responds to an *i*th electric field (Kim, Song, & Yun, 2006; Kim, Yun, & Ounaies, 2006). Such materials are made up of cellulose fibers dissolved in a solvent and cast as a sheet. Thin gold electrodes were deposited on both sides of the cellulose film, and when an electric field was applied across the thickness of the film, it showed a bending deformation. This cellulose film is a kind of electro-active polymer (EAP) (Bar-Cohen, 2004). Cellulose EAP has merits as a smart material in terms of lightweight, dryness, biodegradability, abundance, low price, large displacement output and low actuation voltage. Cellulose EAP material will enable inexpensive and lightweight bio-mimetic actuators, microelectro-mechanical systems (MEMS) devices, smart wallpaper, e-papers, etc. Cellulose EAP material is also promising as biosensors since it is biodegradable, biocompatible, sustainable, capable of broad chemical modification and has high mechanical stiffness and strength. The discovery of an electromechanical coupling effect in wood dates back to 1950 when Bazhenow reported a piezoelectric response in wood (Bazhenow, 1961). Fukada experimentally verified the piezoelectric coefficients of wood, and demonstrated that oriented cellulose crystallites were responsible for the observed shear piezoelectricity (Fukada, 2000). These previous research results imply that cellulose has potential to be used as an electro-active polymer. However, cellulose EAP is very sensitive to humidity, its maximum bending performance was shown at high humidity condition (90% RH), and its performance is degraded quickly with time (Kim, Song, et al., 2006; Kim, Yun, et al., 2006). To overcome the drawbacks, various attempts have

* Corresponding author at: No. 63 ChenLin Street, HeDong District, Postcode 300160 Tianjin, China. Tel.: +86 22 24538385; fax: +86 22 24528187.
*E-mail address:* caizhijiang@hotmail.com (Z. Cai).

0144-8617/$ – see front matter © 2011 Elsevier Ltd. All rights reserved.
doi:10.1016/j.carbpol.2011.08.038

been made to improve cellulose EPA's performance. As one of the approaches, polypyrrol and polyaniline conductive polymers were coated on cellulose EAP (Deshpande, Kim, & Yun, 2005a, 2005b). The conductive polymer-coated cellulose EAP exhibited a large displacement output, but it was still sensitive to humidity and the degradation was not improved. Another attempt was to mix carbon nanotubes (CNT) with cellulose (Yun & Kim, 2007; Yun, Zhao, Wang, & Kim, 2006). This CNT-mixed cellulose EAP can increase the mechanical power output and resonance frequency, but it was also still sensitive to humidity. So, preparing cellulose EAP with high performance in room humidity condition is required to make this smart material useful in future practical application.

Poly(3-hydroxybutyrate) (PHB) is saturated aliphatic polyester synthesized and accumulated by a variety of bacteria as a reserve energy source (Zahra et al., 2009). PHB isolated from the bacteria is a partially crystalline polymer. PHB has many remarkable characteristics such as biodegradability, biocompatibility, optical activity and anticruor (Savenkova et al., 2000; Zhao, Deng, Chen, & Chen, 2003). It is a truly biodegradable material suitable for two promising applications: one is as a viable candidate for relieving environment concerns caused by disposal of non-degradable plastic; the other is to provide new-type biomedical materials. At the same time, PHB also has piezoelectricity and it can be used as electro-active material.

In the present research, cellulose/PHB blend film is used to prepare a novel EAP material. We expect that the cellulose/PHB blend EAP shows improved bending performance compared with pure cellulose EAP in terms of free bending displacement output, electrical power consumption and lifetime.

## 2. Materials and methods

### 2.1. Materials

Cotton cellulose (MVE, DPw 7450) was purchased from Buckeye Technologies Co., USA. The poly(3-hydroxybutyrate) (PHB), a white powder sample was kindly provided by Tianjin TianLu Co. Ltd. (China), $M_w$ = 430,000 $M_w/M_n$ = 1.49 (obtained by G.P.C. in chloroform at 30 °C). It was purified by precipitation in *n*-hexane from chloroform solution, subsequently precipitated in methanol from chloroform solution. Hydrochloric acid (36.5–38%) was purchased from Sigma–Aldrich, USA. Trifluoroacetic acid (>99%) was purchased from Daejung Chemical & Metals Co. Ltd. Sodium hydroxide (bead, 98%) was purchased from Samchun Pure Chemical Co. Ltd.

### 2.2. Preparation of cellulose/PHB blend film

Cotton cellulose was cut into small pieces, soaked into water overnight, squeezed and filtered to remove the water. The same process was performed four times with methanol and once with acetone. The treated cotton cellulose and PHB powder were heated under reduced pressure at 110 °C for 2 h. Then cotton cellulose was mixed with PHB powder at 50:50 weight ratios and dissolved in trifluoroacetic acid at room temperature. The transparent cellulose/PHB blend solution was kept in sealed glass bottle for future use. The clear mixture solution was spin-coated on wafer and dried at room temperature for 12 h. To ensure complete elimination of the solvent, the films were then dried at 60 °C for 6 h. Transparent films can be obtained by peeling them off from the wafer. After that, the films were soaked in 1 N NaOH at room temperature for 1 day to remove the acids. They were then washed with running tap water for 8 h, and then immersed in deionized (DI) water for 24 h. Since sodium ions were entirely removed by running water, its concentration in the film was negligible. And then the films were immersed in hydrogen chloride aqueous solution (the concentration of hydrogen chloride is 1%) for 2 h, and then washed with tap water and DI water for 12 h to remove little ionic molecules. And then the films were dried in air for 24 h.

### 2.3. Gold electrode coating

Gold electrodes were deposited on both sides of the cellulose/PHB film by using a physical vapor deposition system. The size of the sample was 15 mm × 40 mm. The thickness of the gold electrodes was so thin (0.1 μm) that the gold electrodes did not significantly affect the bending stiffness of the cellulose/PHB blend film.

### 2.4. Characterization

Scanning electron microscopy images of the film were taken with a microscope (Hitachi S-4200, Japan) to study the morphological difference of the films. The surface and cross-section of the films were sputtered with gold, and then observed and photographed at an accelerating voltage of 15 kV. FT-IR spectra were obtained using a Perkin-Elmer System 2000 FT-IR spectrophotometer. The sample was cut into very little particles and characterized by a Fourier transform infrared spectroscopy for the evaluation of chemical structures. The sample was formed in a KBr pellet. The obtained data were transferred to the PC for the line fitting. X-ray diffraction (XRD) patterns were recorded on an X-ray diffractometer (D/MAX-2500, Rigaku), by using Cu Kα radiation at 40 kV and 30 mA. The diffraction angle ranged from 5° to 40°. Differential scanning calorimetry (DSC, Model NETZSCH STA 409) was performed under a continuously renewed nitrogen atmosphere (flow rate, 20 mL/min). The sample was heated from room temperature to 400 °C at the heating rate of 10 °C/min. Tensile test specimens were prepared by cutting the membranes to 10 mm wide and 65 mm long strips using a precise cutter. Young's modulus of samples were found from the tensile test results conducted according to ASTM D-882-97 as a standard test method for tensile elastic properties of thin plastic sheeting. Tensile test was done on a universal testing machine in ambient condition. Two ends of the specimens were placed between the upper and lower jaws of the instrument, leaving a length of 50 mm of the film in between the two jaws. Extension speed of the instrument was 2 mm/min. For each test, four samples were used to calculate the average value and derivations. Dynamic mechanical analysis (DMA) was conducted in tension mode on a DMA 2980. Temperature scans were run from −40 °C to 50 °C at a heating rate of 2 °C/min with a frequency of 1 Hz. Five replicates were tested for each sample.

### 2.5. Bending performance

The bending performance of the cellulose/PHB blend EAP was evaluated in terms of bending displacement, electrical power consumption and durability with respect to the actuation frequencies, voltages, and time variations. The test was conducted in the bending displacement measurement system, which consists of a high precision laser doppler vibrometer (LDV) (Keyence, LK-G3001(P)V), a current probe (Tektronix, TCPA300), and a function generator (Agilent, 33220A). A sample is supported vertically in air. The function generator sends out the excitation AC voltage. The input signal generated from the function generator is applied to the sample and it produces a bending deformation. The bending displacement of the sample is measured by the high precision LDV and the signal is converted to the displacement through the computer. Simultaneously, the current probe measures the input current supplied from the function generator. The measured current signal is also analyzed simultaneously by the computer.

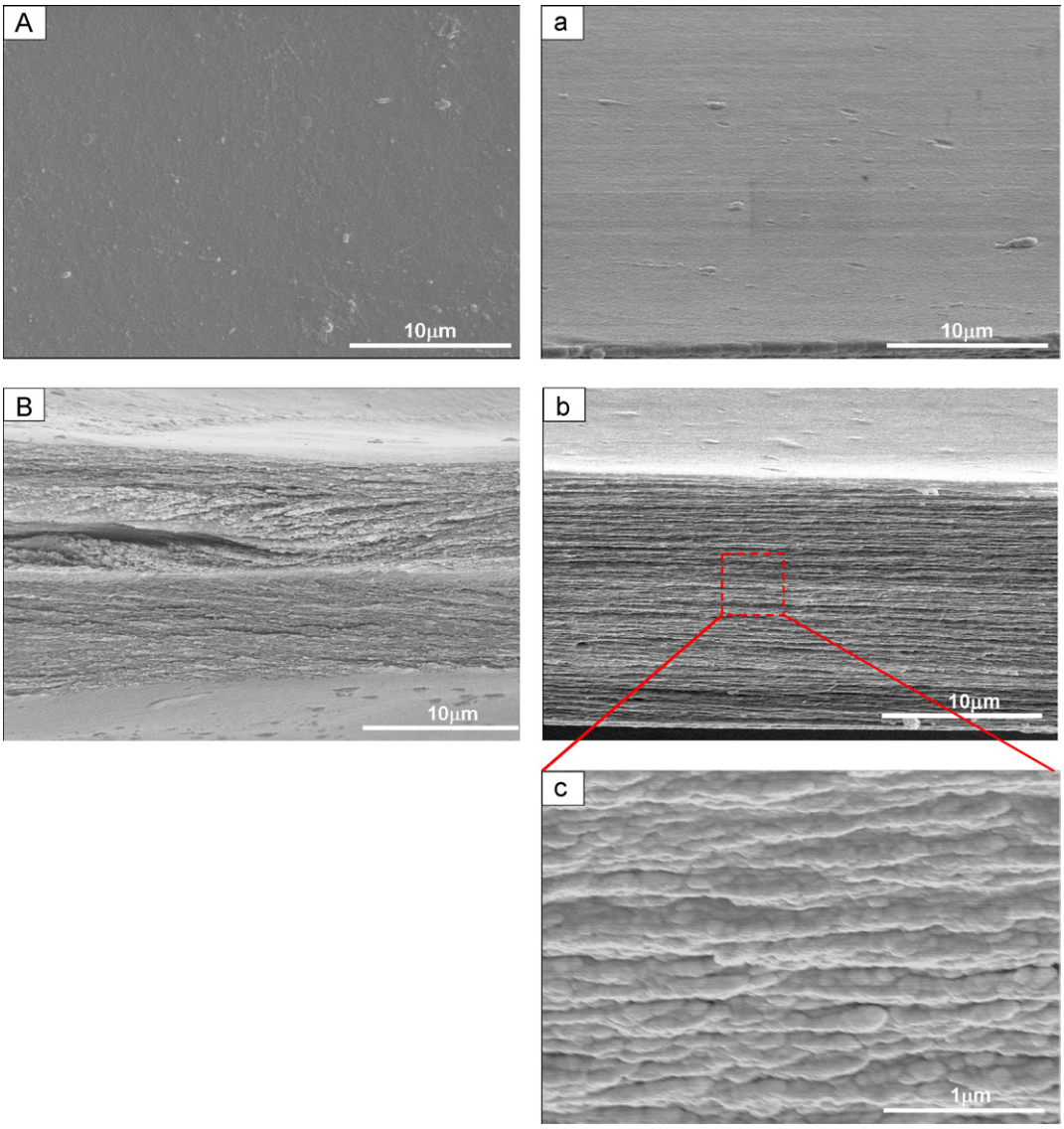


**Fig. 1.** SEM images of cellulose (A and B) and cellulose/PHB blend (a–c) (A, a: surface morphology; B, b: cross-sectional morphology, c: high magnification for selected region).

## 3. Results and discussion

### 3.1. SEM images

SEM observation can give information of the morphological change and miscibility. Cellulose/PHB blend EAP was made using solution casting. The SEM images of the surface and cross-section of the cellulose and cellulose/PHB blend EAP are shown in Fig. 1. Since the gold layer was so thin, it can be assumed that the surface SEM images can represent the true surface morphology. For pure cellulose film, the surface morphology is very uniform and smooth; the cross-section morphology is typical layer-by-layer structure (Fig. 1B). For cellulose/PHB blend EAP, the surface is rather smooth and no phase separation can be observed. A lamination structure can be observed from the cross-section images (Fig. 1b). This kind of structure has been reported previously as nematic ordered cellulose (Kondo, Togawa, & Brown, 2001). Generally, we can calculate the average thickness of each layer using SEM images with high magnitude (the SEM images are not all presented). For pure cellulose EAP, the average thickness of each layer is about $50 \pm 4$ nm, whereas for cellulose/PHB blend EAP, the average thickness of each layer increases to $200 \pm 30$ nm (Fig. 1c). The reason might be due to the fact that since the process of cellulose regeneration and PHB formation happen simultaneously, PHB molecules and cellulose molecules can interpenetrate with each other to form a uniform cellulose/PHB blend. Thus, no obviously phase separation can be observed. All these results indicate that cellulose and PHB were blended well. Also, this good miscibility guarantees the uniformity and stability of the bending performance.

### 3.2. FT-IR

Fig. 2 depicts the FT-IR spectra of PHB, cellulose and cellulose/PHB blend film. For pure PHB (Fig. 2a), the peak at 3433 $cm^{-1}$ refers to hydroxyl end groups. Peaks at 2973 $cm^{-1}$, 2889 $cm^{-1}$ and 2741 refer to C–H stretching vibration. A sharp and steep band observed at 1726 $cm^{-1}$ is assigned to C=O stretching vibration. The peak at 1283 $cm^{-1}$ refers to C–O stretching vibrations. In the case of pure cellulose (Fig. 2b), a broad band at 3450 $cm^{-1}$ is attributed to O–H stretching vibration. Band at 2820 $cm^{-1}$ represents the aliphatic C–H stretching vibration. A sharp and steep band observed at 1080 $cm^{-1}$ is due to the presence of C–O–C stretching vibrations. Spectra obtained for cellulose/PHB blend (Fig. 2c) display basically the bands observed for the two individual components. Only the

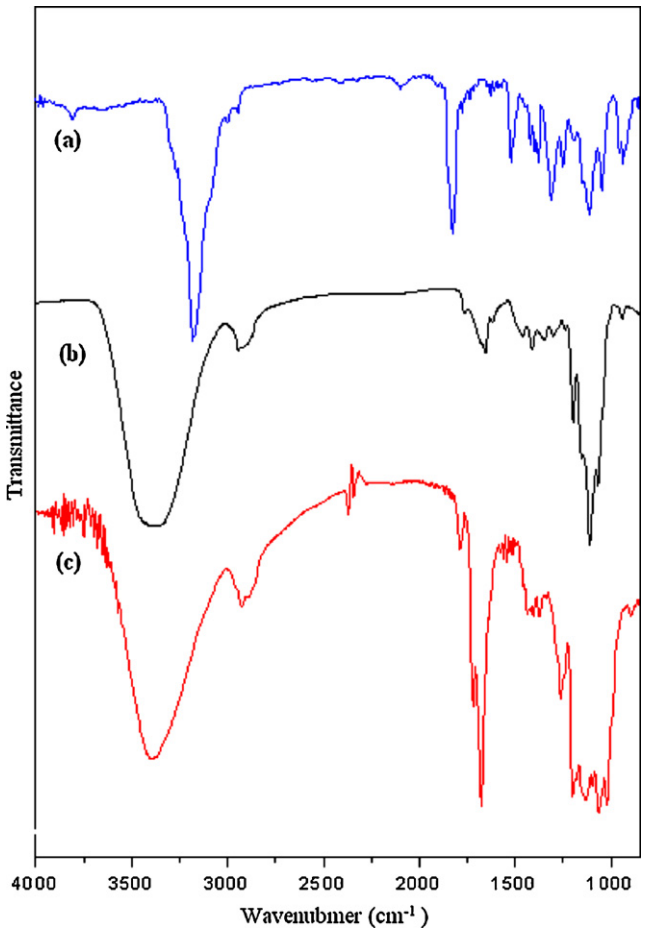


**Fig. 2.** FTIR spectra of PHB (a), cellulose (b) and cellulose/PHB blend (c) film.

frequency is shifted to lower region. As we known, the frequency difference is considered as a measure of the average strength of the intermolecular hydrogen bond (Liang, Wu, Zhang, & Xu, 2008). The frequency difference between that intermolecular interactions between the two polymers occur. However further measurements such as Raman spectroscopy would be necessary to clarify this.

### 3.3. XRD analysis

Fig. 3 shows X-ray diffraction patterns of cellulose, PHB and cellulose/PHB blend films. Regarding the crystalline structure of cellulose, it is known to be classified into four crystallization types,

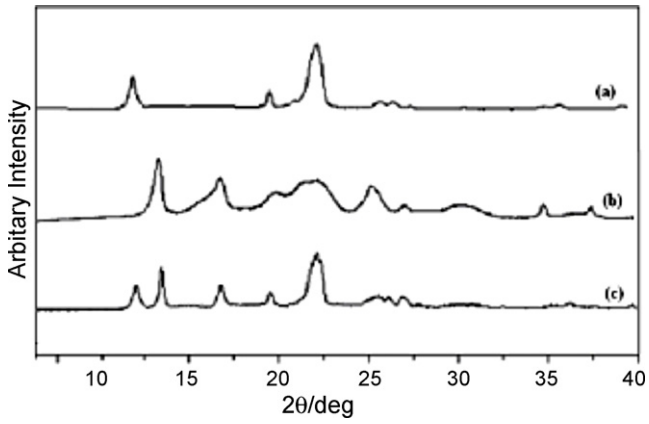


**Fig. 3.** XRD patterns of cellulose (a), PHB (b) and cellulose/PHB blend (c).

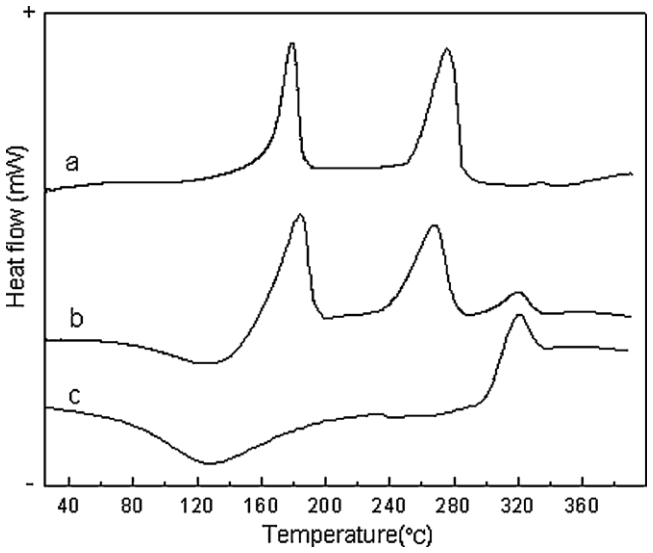


**Fig. 4.** DSC curves of PHB (a), cellulose/PHB blend (b) and cellulose (c).

viz. celluloses I–IV, and their crystalline structure are able to be transformed from one type to another (Jung, Benerito, Berni, & Mitcham, 1977). As seen from Fig. 3a, for pure cellulose three peaks located at 12.1°, 19.8° and 22° assigned to (1 1 0), (1 $\bar{1}$ 0), and (2 0 0) can be observed, which represent cellulose II crystalline structure. Yokouchi, Chatani, Tadokoro, Teranishi, and Tani (1973) had reported that PHB crystallizes in an orthorhombic lattice structure ($P2_12_12_1$: $a = 0.576$ nm, $b = 1.320$ nm and $c = 0.596$ nm (fiber axis), α-form) with their chains in the left 2/1 helix. Characteristic XRD diffractiongram of pure PHB film is given in Fig. 3b, which agrees with the report in the literature. Two strong scattering intensity peaks are detected at $2\theta$ value of 13° and 17° assigned to be (0 2 0) and (1 1 0) of the orthorhombic unit cell respectively. For cellulose/PHB blend film, diffraction patterns show the PHB characteristic peaks with a decrease intensity and cellulose II characteristic peaks (Fig. 3c).

The crystallinity index for cellulose obtained form X-ray diffraction data was calculated according to the literature method (Segal, Creely, Martin, & Conrad, 1959). This method is fast and easy. It uses the height of the (2 0 0) peak and the minimum between (2 0 0) and (1 1 0) peaks, assuming that intensity of (2 0 0) represents both crystalline and amorphous parts while the minimum intensity at the mentioned location is for amorphous part only.

$$CrI = \frac{I_{(200)} - I_{(am)}}{I_{(200)}} \quad (1)$$

where $CrI$ is the crystallinity index, $I_{(200)}$ is the intensity at (2 0 0) peak ($2\theta = 22°$) and $I_{(am)}$ is the intensity at the minimum between (1 1 0) and (2 0 0) peak. The estimated crystallinity index of the cellulose is 65% and for cellulose/PHB blend it is 52%. That result indicates that the crystallinity index of cellulose in the cellulose/PHB blend film decreases approximately 10% by blending the PHB. We suggest that it might be due to the strong intermolecular reaction between cellulose and PHB, which makes the cellulose molecular chains difficult to orientation.

### 3.4. DSC test

To further investigate the crystallinity of the cellulose/PHB blend film, we conducted differential scanning calorimetry (DSC) study. DSC thermograms of the cellulose/PHB blend film with pure PHB and cellulose for comparison are displayed in Fig. 4. For pure PHB, two sharp endothermic peaks located at 173 °C and 278 °C can

be observed. These two peaks are attributed to melting transition of the PHB crystalline and thermal decomposition of PHB molecular chain. In the case of pure cellulose, a broad peak is observed at 127 °C, which should be due to the recrystallization of cellulose during the heating process. And a small peak located at 320 °C is found which is attributed to the melting transition of the cellulose crystal. For cellulose/PHB blend, the DSC curve has some changes. The melting temperature of PHB is shifted to higher temperature while the thermal decomposition temperature of PHB is shifted to lower temperatures. The recrystallization and melting temperature of cellulose are not changed but the peaks area become smaller, which means the crystallinity of cellulose decreases in the blend compared with pure cellulose. These results indicate that the strong intermolecular reaction between cellulose and PHB occurs during the solution blending as we suggest in XRD discussion.

### 3.5. Tensile test

To investigate the mechanical characteristics of cellulose/PHB blend film, the tensile test was performed according to ASTM D-882-97 standard test method. The tensile strength, elongation at break and Young modulus of the cellulose, PHB and cellulose/PHB blend are shown in Fig. 5. Compared with the values observed for pure cellulose, the tensile strength, elongation at break and the Young's modulus experiment a small decrease with the addition of PHB. Pure cellulose and PHB present a tensile strength of 112 MPa, 25 MPa, elongation at break of 8.0%, 4.5% and Young's modulus of 4.12 GPa, 0.6 GPa, respectively. The values observed for cellulose/PHB blend are 74 MPa for the tensile strength, 7.2% for elongation at break and 2.5 GPa for the Young's modulus. This behavior may be associated with the result that the crystallinity of cellulose decreases due to irregular structures caused by strong interactions between cellulose and PHB chains with PHB blending. Meanwhile, the Young's modulus values can be used to calculate the stiffness and resonance frequency of bending performance for the samples.

### 3.6. DMA test

The dynamic mechanical properties of cellulose/PHB blend was examined by DMA and compared with pure cellulose and PHB. The loss modulus curves and tan $\delta$ curves for pure PHB, cellulose and cellulose/PHB blend are shown in Fig. 6. For pure PHB, glass relaxation peak can be observed on both curves around 25 °C. For pure cellulose, the loss modulus is much lower than pure PHB since it is in the glassy state below 50 °C. The relaxation peak observed in tan $\delta$ curve around −25 °C is assigned to β-relaxation. After blending cellulose with PHB, loss modulus for blend increases about one magnitude and both the β-relaxation of cellulose and glass relaxation of PHB are shifted to lower temperature. Lower transition temperature indicates that decreased energy is required for the chain to perform the motion. The change in energy requirement is likely due to the restraint of cellulose and PHB chains caused by the strong intermolecular reaction between these two polymers.

### 3.7. Bending displacement

The bending displacement of pure cellulose EAP and cellulose/PHB blend EAP under AC activation voltage was measured at the tip of the samples with the laser vibrometer. The test was performed as a function of frequency under different activation voltage at room condition. Fig. 7b shows the typical actuation behavior of cellulose/PHB blend EAP under different excitation voltage (peak to peak, ranged from 3 V to 7 V) at room condition (25 ± 0.5 °C and 30 ± 5% RH) and pure cellulose EAP (Fig. 7a) used as comparison. As seen in Fig. 7, when the actuating voltage increases, the

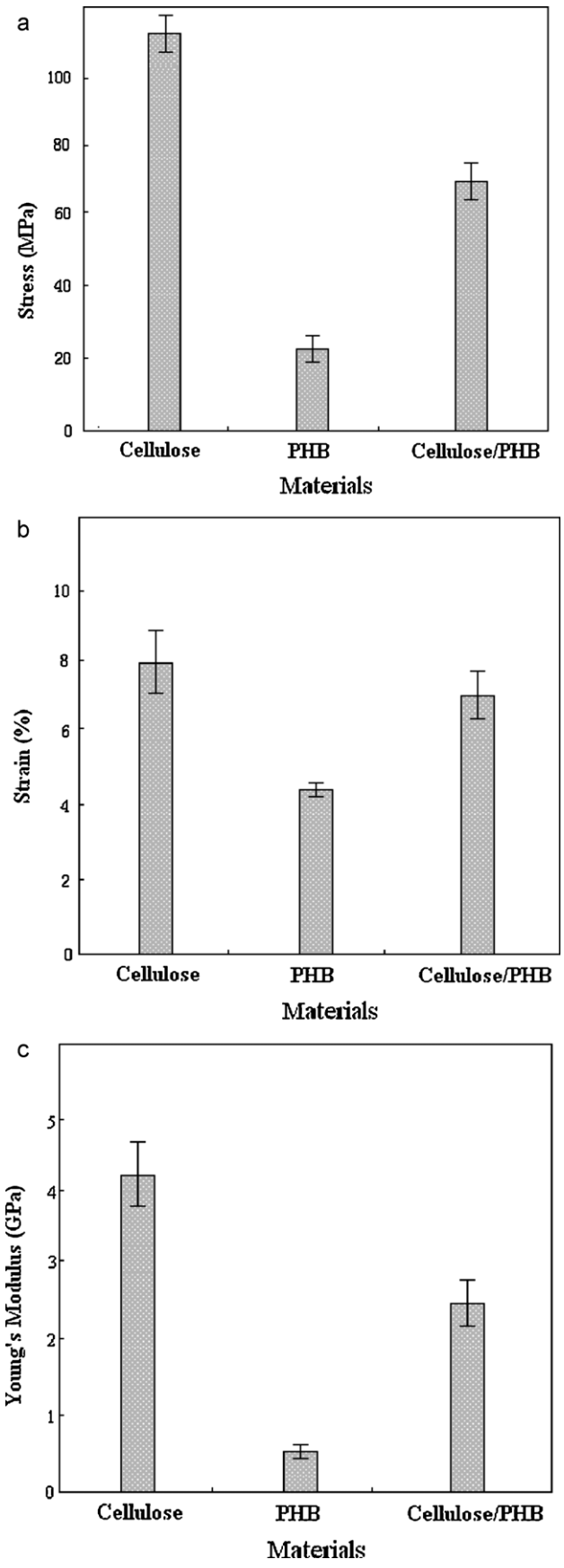


**Fig. 5.** Tensile strength (a), elongation at break (b) and Young's modulus (c) of cellulose, PHB and cellulose/PHB blend.

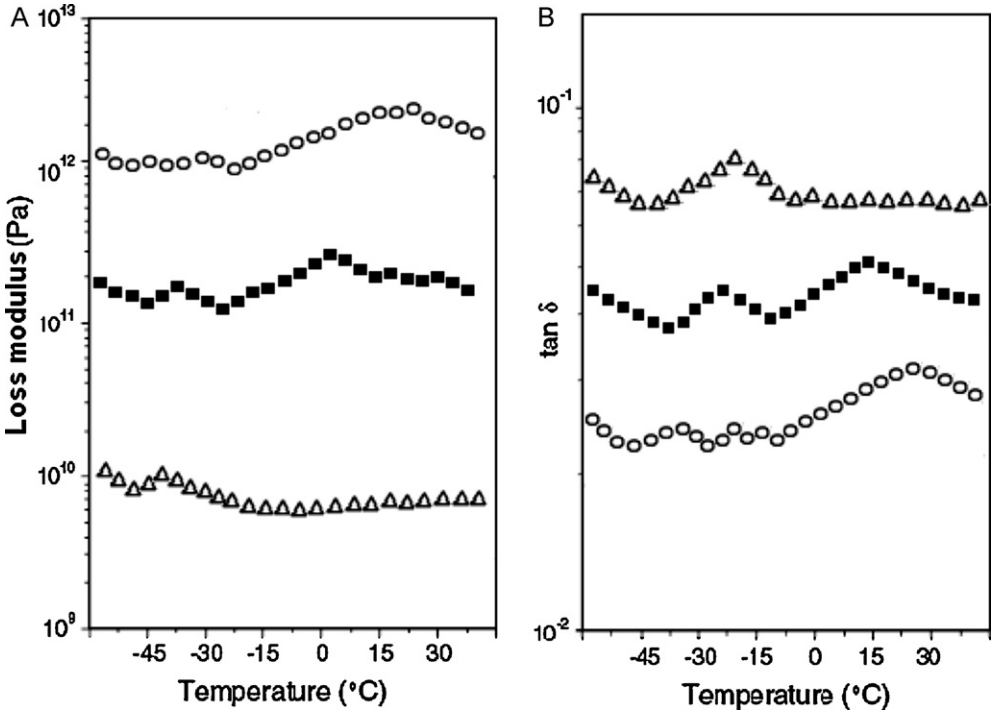


**Fig. 6.** Loss modulus (A) and tan $\delta$ (B) as a function of temperature (◯: PHB, △: cellulose, ■: cellulose/PHB blend).

bending displacement tends to increase for both cellulose and cellulose/PHB blend EAP. The maximum bending displacement values of 1.32 mm is achieved for cellulose/PHB blend EAP at actuating voltage of 7 V at room humidity conditions, which is higher than that of pure cellulose EAP (0.92 mm). We think the increase of bending displacement of cellulose/PHB blend EAP might be attributed to the piezoelectricity of PHB. The resonance frequency is also shifted from 5.5 Hz for pure cellulose EAP to 5.0 Hz for cellulose/PHB blend EAP. The resonance frequency of EAP can be theoretically calculated based on the classical beam theory (Rao, 1990). Supposing the gold electrode layer is so thin (~100 nm) that its stiffness is negligible, the resonance frequency of the EAP is proportional to the root of Young's modulus (Tahhan, Truong, Spinks, & Wallace, 2003). In this case, the main reason for resonance frequency decrease is the Young's modulus decrease with blending PHB in the blend. The decrease in the stiffness also can result in a larger bending displacement.

To investigate the humidity effect on the cellulose/PHB blend EAP, we perform the bending displacement test under the different relative humidity levels, such as 50%, 60%, 70%, 80% and 90%. All tests were performed under room temperature at $25 \pm 0.5\,^{\circ}C$. Fig. 7c shows the measured maximum bending displacements at different relative humidity levels at 7 V and resonance frequency. For pure cellulose EAP, its maximum bending displacement is very sensitive to environmental humidity condition. At low humidity level (room humidity), its maximum bending displacement is very low. However, with humidity condition increasing, its maximum bending displacement increases almost linearly. The highest value is achieved at 90% humidity condition in this test. For cellulose/PHB blend EAP, the humidity sensitiveness of bending displacement becomes less compare humidity.

### 3.8. Electrical power consumption

Fig. 8A and B shows the electrical power consumption of pure cellulose EAP and cellulose/PHB blend EAP at the ambient condition. With actuation voltage increasing from 3 V to 7 V, the electrical power consumption level is increased from about 20 mW to 70 mW for pure cellulose EAP and from 35 mW to 140 mW for cellulose/PHB blend EAP, respectively. Under low actuation voltage (such as 3 V and 4 V), the electrical power consumption variation with the frequency is very low, less than 5 mW for both pure cellulose and cellulose/PHB blend EAP. While for high actuation voltage (such as 6 V and 7 V), the electrical power consumption variation with the frequency becomes big. However, the electrical power consumption of cellulose/PHB blend EAP is 104 mW and 119 mW when it is excited with 6 V and 7 V at resonance frequency. This value is higher than that of pure cellulose EAP, which is about 42 mW and 56 mW. The increased electrical power consumption might be due to the increased piezoelectricity associated with blended PHB. Although the electrical power consumption of the cellulose/PHB blend EAP is higher than pure cellulose EAP, the net electrical power consumption calculated by diving by electrode area is about 17 and 20 mW $cm^{-2}$ for 6 V and 7 V at 5 Hz. These values are lower than that of the microwave power limit that can damage living organs.

### 3.9. Lifetime

The lifetime is one of the important characteristics of EAP. One drawback of cellulose EAP is that its performance degrades rapidly with time, especially under high humidity condition. It might be associated with solvent residues, electrolytic gas or electrode damage. The lifetime was tested as the bending displacement variation with time at resonance frequency and actuation of 7 V at room humidity condition. Fig. 8C shows the lifetime result of cellulose/PHB blend EAP as comparison with pure cellulose EAP. As seen in Fig. 8C, the initial bending displacement is about 0.95 mm for pure cellulose EAP and kept stable at this value for about 60 min. Then, it decreases almost linearly. After actuating for 6 h, its bending displacement reduces to 0.65 mm, which remain only 68% of initial value. However, for cellulose/PHB blend EAP, the initial

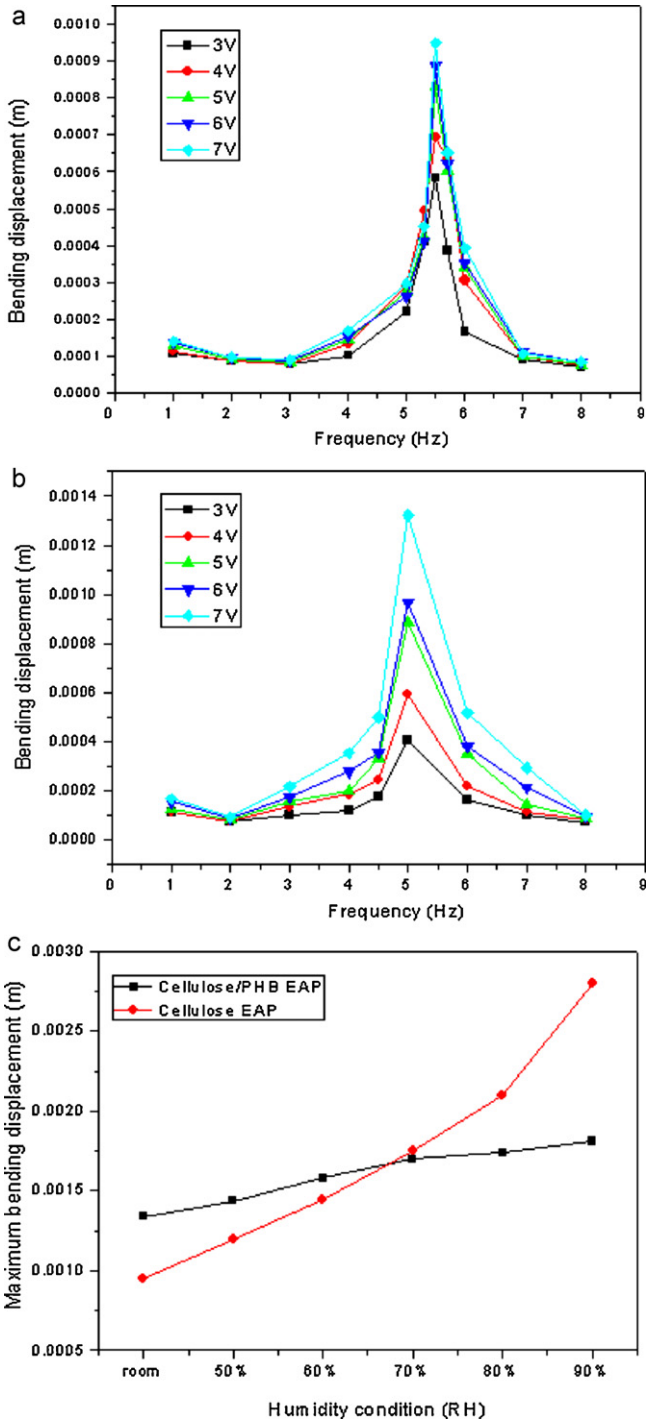


**Fig. 7.** Bending displacements of pure cellulose EAP (a) and cellulose/PHB blend EAP (b) at room condition and maximum bending displacements (c) at different humidity condition.

bending displacement is about 1.3 mm and then drops to 1.125 mm in few minutes. After that, the bending displacement increases slowly and saturates to 1.225 mm after about 1 h. For the next 2 h, the bending displacement is very stable. After that, the bending displacement decreases slowly. After actuation for 10 h, the bending displacement reduces to 0.96 mm. The bending displacement output loss is about 26%. The initial drop of the bending displacement may be associated with initial aging of the material for the electrical actuation. Nevertheless, this cellulose/PHB blend EAP shows a better lifetime in room humidity condition.

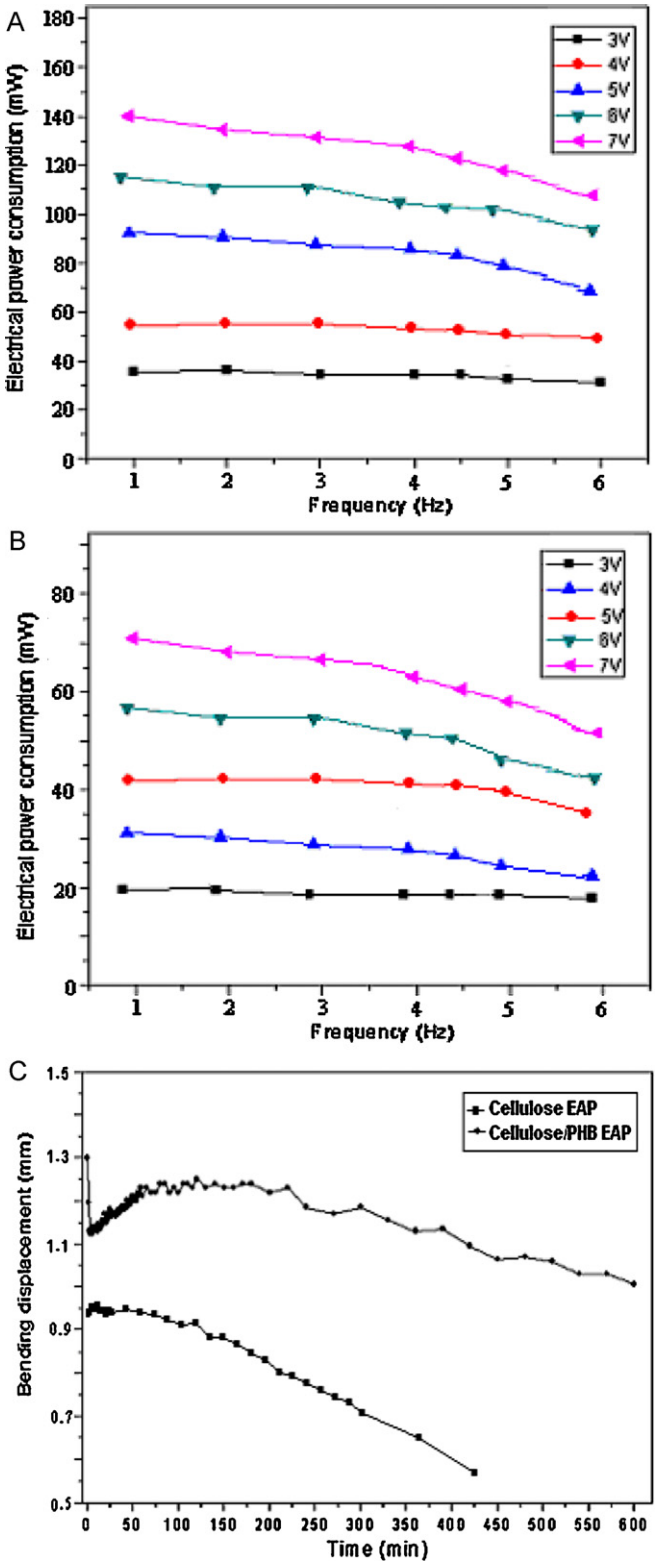


**Fig. 8.** Electrical power consumption (A: pure cellulose EAP; B: cellulose/PHB blend EAP) and lifetime test (C) at room condition.

## 4. Conclusion

Cellulose/PHB blend EAP was prepared by dissolving cellulose and PHB with weight ratio 50:50 in trifluoroacetic acid as co-solvent followed by air drying at ambient. Its characteristics were investigated by SEM, FT-IR, XRD, DSC, DMA and tensile test. SEM

images show that cellulose and PHB has good miscibility and the cellulose/PHB blend has uniform structure. FTIR, XRD and DSC test results confirm the existence of cellulose and PHB in the blend. In addition, a decrease in crystallinity and mechanical properties is observed for cellulose/PHB blend compared with pure cellulose. The bending performances such as bending displacement, electrical power consumption and lifetime were evaluated under AC voltage at an ambient condition by changing the actuation voltage, frequency and time. The bending displacement of the cellulose/PHB blend EAP increases with the actuating voltage increasing. The maximum bending displacement of 1.32 mm, which is higher than that of pure cellulose EAP, is achieved at actuating voltage of 7 V and the resonance frequency of 5 Hz. As for electrical power consumption, although the value is higher than that of pure cellulose EAP it is still lower than the safety limit of microwave which may damage living organs. In terms of durability, bending lifetime for 10 h only lose about 26% performance degradation at room humidity level, which means this novel cellulose/PHB blend EAP has excellent durability and is more promising for potential application in sensors and actuators than pure cellulose EAP.

## Acknowledgements

This work was supported by Tianjin Municipal Natural Science Foundation under the contract of 11JCYBJC02500. We also want to make an acknowledgement to the Creative Research Center for EAPap Actuator, Inha University.

## References

Bar-Cohen, Y. (2004). *Electroactive polymer (EAP) actuators as artificial muscles: Reality, potential, and challenges*. Bellingham: SPIE Press.

Bazhenow, V. A. (1961). *Piezoelectric properties of woods*. New York: Consultants Bureau Enterprise Inc. (p. 130).

Deshpande, S. D., Kim, J., & Yun, S. (2005a). Studies on conducting polymer electroactive paper actuator: Effect of humidity and electrode thickness. *Smart Material and Structure*, *14*, 876–880.

Deshpande, S. D., Kim, J., & Yun, S. (2005b). New electro-active paper actuator using conducting polypyrrole: Actuation behavior in $LiClO_4$ acetonitrile solution. *Synthetic Metals*, *14*, 53–58.

Eichhorn, S. J., Baillie, C. A., Zafeiropoulos, N., Mwaikambo, L. Y., Ansell, M. P., Dufresne, A., et al. (2001). Review current international research into cellulosic fibres and composites. *Journal of Materials Science*, *36*(9), 2107–2131.

Fukada, E. (2000). History and recent progress in piezoelectric polymers. *IEEE Transactions on Ultrasonics, Ferroelectrics and Frequency Control*, *47*, 1277–1285.

Jung, H. Z., Benerito, R. R., Berni, R. J., & Mitcham, D. (1977). Effect of low temperatures on polymorphic structure of cotton cellulose. *Journal of Applied Polymer Science*, *21*, 1981–1988.

Kim, J., Song, C., & Yun, S. (2006). Cellulose based electro-active paper: Performance and environmental effects. *Smart Materials and Structure*, *15*, 719–725.

Kim, J., Yun, S., & Ounaies, Z. (2006). Discovery of cellulose as a smart material. *Macromolecules*, *39*, 4202–4206.

Klemm, D., Heublein, B., Fink, H.-P., & Bohn, A. (2005). Cellulose: Fascinating biopolymer and sustainable raw material. *Angewandte Chemie International Edition*, *44*, 3358–3393.

Kondo, T., Togawa, E., & Brown, R. M., Jr. (2001). Nematic ordered cellulose: A concept of glucan chain association. *Biomacromolecules*, *2*, 1324–1330.

Liang, S., Wu, J., Zhang, L., & Xu, J. (2008). High-strength cellulose/poly(ethylene glycol) gels. *ChemSusChem*, *1*(6), 558–563.

Rao, S. S. (1990). *Mechanical vibrations* (2nd ed.). Reading, Massachusetts: Addison-Wesley Publishing Company. (p. 398).

Savenkova, L., Gercberga, Z., Nikolaeva, V., Dzene, A., Bibers, I., & Kalnin, M. (2000). Mechanical properties and biodegradation characteristics of PHB-based films. *Process Biochemistry*, *35*, 573–579.

Segal, L., Creely, J. J., Martin, A. E., & Conrad, C. M. (1959). An empirical method for estimating he degree of crystallinity of native cellulose using the X-ray diffractometer. *Textile Research Journal*, *29*, 786–794.

Tahhan, M., Truong, V. T., Spinks, G. M., & Wallace, G. G. (2003). Carbon nanotube and polyaniline composite actuator. *Smart Materials and Structure*, *12*, 626–632.

Takayasu, T., & Fumihiro, Y. (1997). Production of bacterial cellulose by agitation culture systems. *Pure & Applied Chemistry*, *69*(11), 2453–2458.

Yokouchi, M., Chatani, Y., Tadokoro, H., Teranishi, K., & Tani, H. (1973). Structural studies of polyesters: 5. Molecular and crystal structures of optically active and racemic poly (β-hydroxybutyrate). *Polymer*, *14*, 267–272.

Yun, S., & Kim, J. (2007). A bending electro-active paper actuator made by mixing multi-walled carbon nanotubes and cellulose. *Smart Materials and Structure*, *16*, 1471–1476.

Yun, S., Zhao, L. J., Wang, N. G., & Kim, J. (2006). Hybrid electro-active papers of cellulose and carbon nanotubes for bio-mimetic actuators. *Key Engineering Materials*, *324–325*, 843–846.

Zahra, B. M., Ebrahim, V., Ali, H., Shojaosadati, S. A., Ramin, K., & Kianoush, K. D. (2009). Statistical media optimization for growth and PHB production from methanol by a methylotrophic bacterium. *Bioresource Technology*, *100*, 2436–2443.

Zhao, K., Deng, Y., Chen, J. C., & Chen, G. Q. (2003). Polyhydroxyalkanoate (PHA) scaffolds with good mechanical properties and biocompatibility. *Biomaterials*, *24*, 1041–1045.